

## Article

# Pruning Optimization over Threshold-Based Historical Continuous Query

Jiwei Qin, Liangli Ma \* and Qing Liu

College of Electronic Engineering, Naval University of Engineering, Wuhan 430033, China;  
18602706401@163.com (J.Q.); qing@alumni.hust.edu.cn (Q.L.)

\* Correspondence: maliangli@163.com

Received: 4 March 2019; Accepted: 18 May 2019; Published: 19 May 2019



**Abstract:** With the increase in mobile location service applications, spatiotemporal queries over the trajectory data of moving objects have become a research hotspot, and continuous query is one of the key types of various spatiotemporal queries. In this paper, we study the sub-domain of the continuous query of moving objects, namely the pruning optimization over historical continuous query based on threshold. Firstly, for the problem that the processing cost of the Mindist-based pruning strategy is too large, a pruning strategy based on extended Minimum Bounding Rectangle overlap is proposed to optimize the processing overhead. Secondly, a best-first traversal algorithm based on E3DR-tree is proposed to ensure that an accurate pruning candidate set can be obtained with accessing as few index nodes as possible. Finally, experiments on real data sets prove that our method significantly outperforms other similar methods.

**Keywords:** moving object; historical continuous query; pruning optimization; spatiotemporal index

## 1. Introduction

With the rapid development of mobile networks and positioning technologies, the trajectory data of mobile objects can be more conveniently obtained. For example, the Automatic Identification System is used to report the real-time location information of ships, and the mobile social applications are used to share the real-time location, etc. The trajectory data of mobile objects contains a large amount of information that can be analyzed and mined. By managing the trajectory data of mobile objects through mobile object database [1], a large number of applications based on location services can be promoted, such as geographic information systems, navigation systems, path planning systems, etc. Therefore, the performance of a mobile object database will determine the service capabilities that the location-based applications can provide.

In the past ten years, the research on mobile object database has achieved a lot of results, covering all aspects of data storage, management, query, and mining. Mobile object query is one of the key technologies of a mobile object database. In different scenarios, various types of query operations are needed to provide service support. Research on how to provide high-performance queries is the key to improving the service capability of a mobile object database. Therefore, it is important to implement a query operation that can accurately return the results in a short time. With the gradual deepening of research, people not only consider the spatial information of the moving object when querying, but also temporal information will be taken into account. At this stage, the query operations for the moving object include spatiotemporal range query, trajectory similarity query, neighbor query, threshold-based query [2], etc. We consider the following query requests for the historical trajectory data:

1. Find which ships were within one nautical mile from the berth  $O_1$  at any time instance of the time period from 10:00 on 11 November 2015 to 10:00 on 12 November 2015.

- Find which ships were within one nautical mile from the ship  $O_2$  at any time instance of the time period from 8:00 on 12 November 2015 to 8:00 on 13 November 2015.

The above two queries require the query results at any time instance of the query time period, wherein the query request (1) takes a static object as the reference, and the query request (2) takes a moving object as the reference, both of which can be characterized as continuous queries [3]. However, there is a certain difference between these continuous queries and the traditional continuous ones. The traditional continuous query submits the query request to the database at once and remains active, and the query results are periodically returned until the predetermined query lifetime ends. While the query requests (1) and (2) demand the database to return all query results at once. It can be seen that these continuous queries face a greater data processing scale challenge than the traditional ones. In addition, we can see from the query conditions that the above query requests are constrained by the spatial distance threshold, so we call them threshold-based historical continuous queries (THC queries).

Figure 1 displays an example of THC query, where  $T_q$  is the historical trajectory of the query moving object  $O_q$ , and  $T_1$ ,  $T_2$ , and  $T_3$  are the historical trajectories of the moving objects  $O_1$ ,  $O_2$ , and  $O_3$ , respectively, and the query time interval is  $(t_1, t_4)$ , the distance threshold is  $d$ . As time goes by, the position of the moving object will change continuously. Hence, the query time interval can be subdivided into a plurality of smaller time segments, and the query results in each time segment are not the same. As Figure 1 shows, the results are  $O_2$  and  $O_3$  at the time interval  $(t_1, t_3)$ ,  $O_1$ ,  $O_2$  and  $O_3$  at time instance  $t_3$ ,  $O_1$  and  $O_2$  at the time interval  $(t_3, t_4)$ .

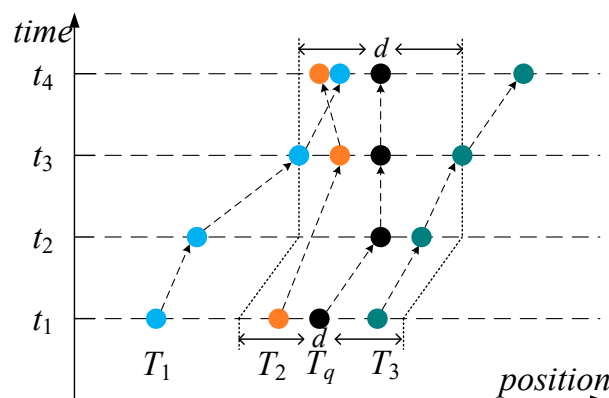


Figure 1. Example of threshold-based historical continuous (THC) query.

THC queries can be processed by the classic “pruning-refinement” method [4]. In the pruning step, a certain pruning strategy is used to roughly check whether the trajectory data in the moving object database satisfies the constraint condition, and the trajectory data that does not match the condition is eliminated, and finally, a candidate set of trajectory data is obtained. The entire pruning process is usually performed by traversing a spatiotemporal index. In the refinement step, the candidate set is further filtered by the distance calculation, and the results that finally satisfy the query condition are returned to the user.

In the above process, the pruning step has a decisive influence on the overall query performance. This is because, first, the time overhead of pruning is an important part of the overall query time. If the pruning strategy can be optimized, and the processing time can be reduced, the overall query performance will undoubtedly be improved effectively. Second, the candidate set of pruning directly affects the performance of refinement. The closer the candidate trajectory data generated by pruning is to the final result, the less the number of trajectory distance calculations required in the refinement step, and the I/O times and the calculation time required for the query can be reduced effectively. In view of this, in order to achieve efficient query performance, we optimized the pruning step of THC

queries. First, the pruning strategy based on extended Minimum Bounding Rectangle (MBR) overlap is proposed to reduce the processing overhead of a single pruning check. Secondly, we designed an extended 3DR-tree [5] structure called E3DR-tree to the index query object, and based on this, we implemented a best-first traversal algorithm, so that an accurate pruning candidate set was obtained with accessing as few nodes as possible in the traversal of the indexes.

Our main contributions can be summarized as follows:

- We propose a pruning strategy based on extended MBR overlap to optimize the single pruning check, thereby effectively reducing the processing time.
- We introduce a best-first traversal algorithm based on E3DR tree, to obtain a precise pruning candidate set for refinement processing under the premise of effectively controlling the number of accessed nodes when traversing the indexes.
- We evaluate our method with the dataset of ship trajectory, the experimental results verify the efficiency.

Section 2 introduces the related work. The background is introduced in Section 3. The method of pruning optimization is described in Section 4. Section 5 provides an experimental study of our method. Finally, we give a brief conclusion in Section 6.

## 2. Related Work

At present, there are many studies on historical continuous query, in addition to threshold-based historical continuous query, it also includes  $k$  nearest neighbor historical continuous query.

Frentzos et al. [6] introduced a depth-first traversal algorithm to support  $k$  nearest neighbor history continuous query and proposes a new line-to-rectangular Mindist (minimum distance) calculation method [7] to improve pruning efficiency. Moreover, they apply the above method in the two index structures of TB-tree [8] and 3DR-tree and verify the feasibility on the real and synthetic data sets.

Güting et al. [9] researched pruning optimization of  $k$  nearest neighbor historical continuous query. They propose an extended 3DR-tree structure to quickly determine the number of candidate trajectories, design a time-based index named BB-tree to achieve high-precision pruning, and based on this, implement a breadth-first large-scale node traversal algorithm to efficiently obtain candidate trajectory data.

Gowanlock et al. [10] conducted a study on threshold-based historical continuous query. In order to reduce the I/O overhead for query processing, they propose a memory-based R-tree structure to index the trajectory data and use a query algorithm based on MBR overlap to process the pruning and refinement. Compared to the first two studies, this study does not focus on the improvement of the algorithm but does a lot of experiments on real datasets to determine the appropriate parameters for the construction of memory-based R-tree. In addition, they also explore the parallelization of query based on OpenMP [11].

Huang et al. [12] propose a new threshold-based historical continuous query operation. For this query operation, a pruning method based on Mindist-Maxdist (minimum distance-maximum distance) and a refinement method based on dynamic time warping are introduced. In addition, this study also discusses the impact of trajectory segmentation on query and evaluates the performance of the query algorithm on the indexes of 3DR-tree, TB-tree and SETI [13], respectively.

With the rapid development of GPU technology, a series of methods [14–16] which use GPU to process the threshold-based historical continuous queries in parallel are proposed. On the one hand, considering that the GPU does not have branch prediction capabilities, these methods avoid using the tree-like structure to index the trajectory data, using the grid structure instead. On the other hand, considering that the GPU memory is limited, different from the snapshot queries taken by the above four methods, these methods divide the trajectory data contained in the mobile object database into multiple batches and iteratively process them.

Aside from the GPU-based methods, the above methods have more or less the following shortcomings: (1) Calculating the values of Mindist or Maxdist requires high computational costs [6,9,12]. (2) During the pruning step, the pruning candidate set generated by taking the whole query trajectory as a whole is not accurate enough [6,12]. Conversely, the pruning method that takes each segment of the query trajectory as a basic unit can obtain a more accurate candidate set, but the number of the accessed nodes is greatly increased [9,10]. In response to these two shortcomings, we will discuss the solutions in detail later.

### 3. Background

The real trajectory of the moving object is a continuous curve in space and time, but the sampling and storage of the trajectory data are carried out in discrete form, this is because the sensor device can only collect and send discrete samples. For example, a taxi equipped with a GPS device reports its position information every 10 s. The discrete position samples of a moving object constitute an ordered sequence of segments. When the sampling frequency is high enough, this sequence of segments can be relatively accurately approximated to the real trajectory of the moving object. Therefore, we used a segment-based data model to represent the trajectory of a moving object, defined as follows:

**Definition 1.** The trajectory  $T$  of a moving object contains a sequence of trajectory segments  $(l_1, l_2, \dots, l_M)$  arranged chronologically. Each trajectory segment  $l$  records the linear motion of a moving object in a time interval, which can be expressed as  $l = \{oid, p_s, p_e, t_s, t_e\}$ ,  $(t_s \leq t_e)$ , where  $oid$  is the identifier of the moving object and it can represent the moving object,  $p_s$  and  $p_e$  respectively represent the spatial position of the moving object at time instance  $t_s$  and  $t_e$ .

According to the data model of trajectory described in Definition 1, the spatial position of the moving object at a certain historical time instance can be obtained by linear interpolation. In the two-dimensional Euclidean space, given a trajectory segment  $l = \{oid, p_s, p_e, t_s, t_e\}$ , the spatial coordinates of  $p_s$  and  $p_e$  are expressed as  $p_s = (q_{s1}, q_{s2})$  and  $p_e = (q_{e1}, q_{e2})$ , let  $loc(t, oid)$  represent the spatial position of  $oid$  at the time instance  $t$ , and  $loc_k(t, oid)$  denote the  $k$ -th dimension coordinate of  $loc(t, oid)$ . For any time instance  $t$  in the time interval  $[t_s, t_e]$ , We compute the value of  $loc_k(t, oid)$  as

$$loc_k(t, oid) = \begin{cases} \frac{q_{ek} - q_{sk}}{t_e - t_s} (t - t_s) + q_{sk} & t_s < t_e \\ q_{sk} & t_s = t_e \end{cases} \quad (1)$$

Using Formula (1), we can calculate the spatial positions of two moving objects at a timestamp, and then obtain the distance between them. In this paper, we used Euclidean distance as the distance metric, let  $d(loc(t, oid_1), loc(t, oid_2))$  denote the distance between  $oid_1$  and  $oid_2$  in the time instance  $t$ , according to the Euclidean distance formula

$$d(loc(t, oid_1), loc(t, oid_2)) = \sqrt{\sum_{k=1}^2 (loc_k(t, oid_1) - loc_k(t, oid_2))^2}. \quad (2)$$

In the two query requests listed in Section 1, the stationary object can be taken as a moving object that stays in a spatial position, so a uniform query definition can be given.

**Definition 2.** Given a moving object  $oid_q$ , a moving object database  $D$ , a time interval  $[t_{sq}, t_{eq}]$ , a distance threshold  $d$ , the historical trajectory  $T_q$  of  $oid_q$  in  $[t_{sq}, t_{eq}]$ , the threshold-based historical continuous query return a collection of query results  $Rs$ , the element  $re$  of  $Rs$  is expressed as a tuple  $(ti, oids)$ , where  $ti$  is a time interval, and  $oids$  is a set of moving objects.  $Rs$  satisfies the following two conditions:

- (1) Given two elements  $re_1, re_2 \in Rs$ , such that  $re_1.ti \cap re_2.ti = \emptyset$  and  $re_1.ti, re_2.ti \subseteq [t_{sq}, t_{eq}]$ .
- (2) Given an element  $re_1 \in Rs$ , a time instance  $t_1 \in re_1.ti$ , a moving object  $oid_1 \in re_1.oids$ , such that  $d(loc(t_1, oid_1), loc(t_1, oid_q)) \leq d$ .

With other words, the time intervals of different  $R_s$  elements do not overlap, and the time interval of any  $R_s$  element must be within the query time interval. Moreover, the distance between each oid in  $R_s.oids$  and  $oid_q$  in any time instance of  $R_s.ti$  must not be greater than the distance threshold  $d$ .

In order to ensure the spatiotemporal query performance of the mobile object database  $D$ , the spatiotemporal index structure such as 3DR-tree and TB-tree can be used to index the trajectory data. Since 3DR-tree has stronger spatiotemporal discriminating ability than TB-tree [17], we used a 3DR-tree called *drtree* to index the trajectory data in  $D$ . 3DR-tree is a straightforward extension of R-tree in the 3D space constituting by  $2 + 1$  (spatial and temporal, respectively) dimensions [6]. It treats time as an extra spatial dimension and uses the trajectory segment as the index entry. Figure 2 shows an example of 3DR-tree.

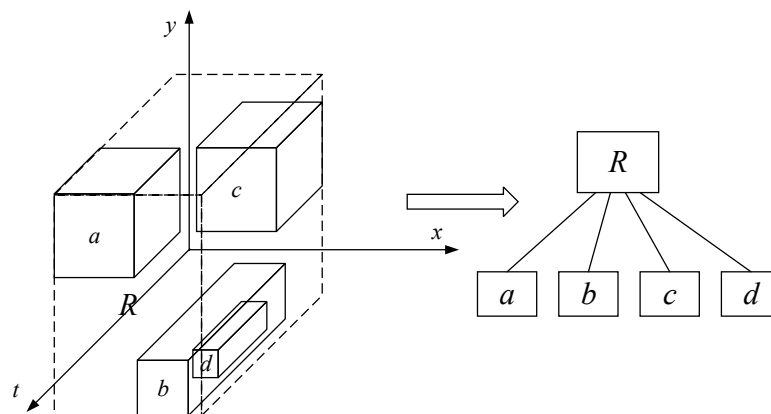


Figure 2. The example of 3DR-tree.

The pruning step is implemented by traversing *drtree*. It starts from the root node of *drtree*, traverses *drtree* from top to bottom, discards the irrelevant *drtree* nodes according to a certain pruning strategy (a *drtree* node refers an index node of *drtree* or a trajectory segment indexed by an index node of *drtree*), and retains the trajectory segments related to the query trajectory  $T_q$  in time and space, finally gets results of candidate trajectory segments.

#### 4. Pruning Optimization

This section describes the pruning optimization method. Section 4.1 introduces the extended MBR-overlap-based pruning strategy, which can effectively reduce the processing overhead of a pruning check. Section 4.2 proposes an index structure for effectively organizing the query trajectory  $T_q$ . Based on the new index structure, the best-first traversal algorithm is introduced in Section 4.3 to ensure a high-precision pruning result with accessing as few nodes as possible. Table 1 lists the frequently used notation in this section.

Table 1. Frequently used notations.

Notation	Description
$TS(x)$	the time interval of $x$
$M(x)$	the spatial MBR of $x$
$Mindist(M_d, M_q)$	minimum distance from spatial area $M_d$ to spatial area $M_q$
$R(x, d)$	the coverage area by extending the MBR of $x$ with the distance threshold $d$
$M_k(x, d)$	the rectangular spatial area by expanding the $k$ -dimensional spatial range of the MBR of $x$ with the distance threshold $d$
$Root(tree)$	the root node of the index <i>tree</i>
$H(N)$	the height from $N$ to the trajectory segment layer of the index

#### 4.1. Extended MBR Overlap Based Pruning Strategy

Given a *drtree* node  $N_d$ , for  $N_d$  and query trajectory  $T_q$ , the basic pruning strategy consists of the following two steps:

1. Check whether the time interval of  $N_d$  overlaps with the time interval of  $T_q$ , if  $TS(N_d) \cap TS(T_q) = \emptyset$ , then  $N_d$  should be pruned.
2. Determine whether the Mindist between the MBR of  $N_d$  and the MBR of  $T_q$  is not greater than the distance threshold  $d$ , if  $Mindist(M(N_d), M(T_q)) > d$ , then  $N_d$  should be pruned.

In the step (2) of the basic pruning strategy, although the Mindist-based method can effectively exclude the trajectory data that does not satisfy the query conditions, its calculation process is complicated and requires a lot of CPU time. When calculating the value of Mindist between  $M(N_d)$  and  $M(T_q)$ , it first determines whether  $M(N_d)$  is overlapped with  $M(T_q)$ , if so, then the value of Mindist is 0. Otherwise, it needs to calculate the minimum distance from any edge of  $M(N_d)$  to  $M(T_q)$ , and chooses the minimum value as the value of Mindist, namely computing the MBR-to-MBR Mindist requires four times of Mindist calculations between a line segment and a rectangle. Moreover, a segment-to-rectangle Mindist calculation is subdivided into six times of distance calculations. As shown in Figure 3, when calculating the minimum distance between the line segment  $L$  and the rectangle  $M$ , it is necessary to calculate two Mindists from each vertex of  $L$  to  $M$  and four Mindists from each vertex of  $M$  to  $L$ , and then select the minimum value among them as the result. Hence, if  $M(N_d)$  does not overlap with  $M(T_q)$ , 24 times of distance calculations are needed to get the value of Mindist between  $M(N_d)$  and  $M(T_q)$ .

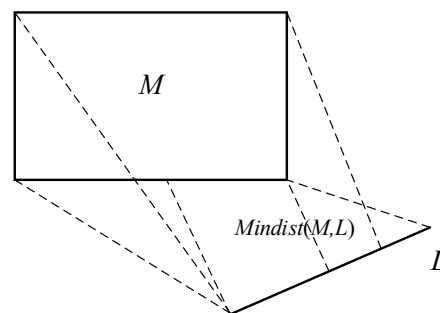


Figure 3. The Mindist between a line segment and a rectangle.

Obviously, the cost of calculating Mindist between two MBRs is expensive, and if the computational cost can be optimized, the query efficiency can be significantly improved. In the process of calculating Mindist, it can be noticed that the cost for checking whether two MBRs overlap is much smaller than the multiple distance calculation, which only needs to compare the spatial positional relationship between the MBR vertices. Suppose the spatial coordinates of the lower left and upper right corners of  $M(N_d)$  are  $(x_{d1}, y_{d1})$  and  $(x_{d2}, y_{d2})$ , the spatial coordinates of the lower left and upper right corners of  $M(T_q)$  are  $(x_{q1}, y_{q1})$  and  $(x_{q2}, y_{q2})$ , if the result of Discriminant (3) is true, then  $M(N_d)$  is overlapped with  $M(T_q)$ . Taking advantage of the low overhead of overlapping calculation, we propose a pruning strategy based on extended MBR overlap to optimize the computational overhead.

$$!(((x_{d2} < x_{q1}) \vee (y_{d1} > y_{q2})) \vee ((x_{q2} < x_{d1}) \vee (y_{q1} > y_{d2}))). \quad (3)$$

First, we use the distance threshold  $d$  to extend the spatial range of  $M(T_q)$ . In the two-dimensional Euclidean space, we can get a coverage area  $R(T_q, d)$  shaped as a rounded rectangle. It is easy to know that if the MBR of a *drtree* node overlaps with  $R(T_q, d)$ , then the Mindist between it and  $M(T_q)$  is no larger than  $d$ . However, since the coverage area of  $R(T_q, d)$  is not a rectangular area, determining whether  $M(T_q)$  overlaps with  $R(T_q, d)$  cannot be based only on the spatial positional

relationship between the vertices, and additional calculations are required. With this in mind, we use the circumscribed rectangle  $M(R(T_q, d))$  of  $R(T_q, d)$  to approximate  $R(T_q, d)$ , if  $M(N_d)$  does not overlap with  $M(R(T_q, d))$ , then it also does not overlap with  $R(T_q, d)$ . Hence, we summarize the Pruning strategy 1.

**Pruning strategy 1.** Given a *drtree* node  $N_d$  and a query trajectory  $T_q$ , a distance threshold  $d$ , if  $M(N_d) \cap M(R(T_q, d)) = \emptyset$ , then  $N_d$  must not contain data related to the query results, and it should be pruned.

Pruning strategy 1 does not involve complex calculations, so it can effectively reduce computational overhead. However,  $M(R(T_q, d))$  increases the coverage area compared to  $R(T_q, d)$ , for such a *drtree* node whose MBR overlaps with  $M(R(T_q, d))$  but does not overlap with  $R(T_q, d)$ , Pruning strategy 1 cannot prune it. For example, in Figure 4, Pruning strategy 1 cannot prune the node  $N_4$ . Therefore, the candidate set generated by using Pruning strategy 1 may contain more irrelevant candidates, which increases the processing overhead of refinement to some extent.

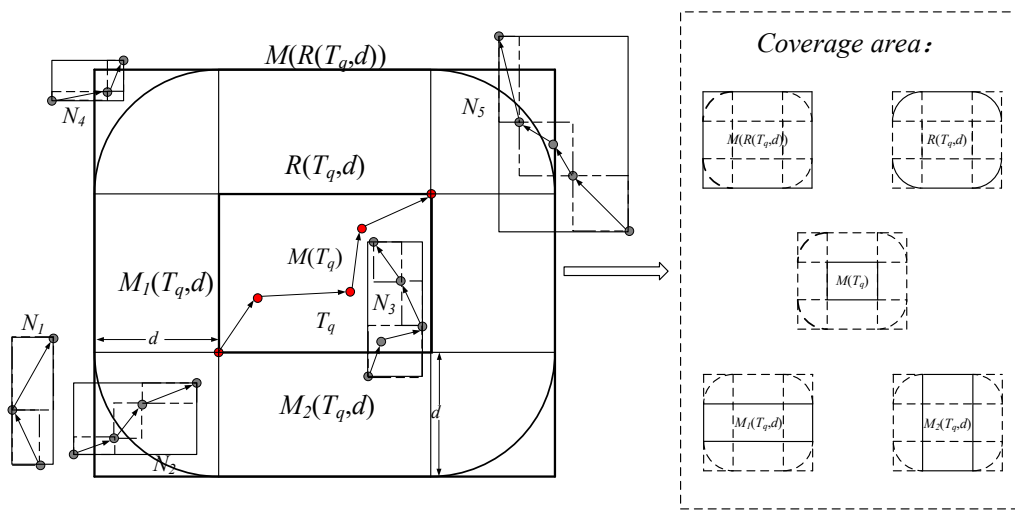


**Figure 4.** Example of extended MBR overlap based pruning strategy.

To overcome this problem, an intuitive method is to further check the *drtree* node that has passed the check of Pruning strategy 1 by calculating Mindist. However, as mentioned earlier, Mindist calculation requires a lot of CPU time and should be avoided during the pruning process. In this regard, we consider the property to be one or more rectangular areas that are fully covered by  $R(T_q, d)$ , if  $M(N_d)$  overlaps with any of them, then  $\text{Mindist}(M(N_d), M(T_q)) \leq d$ . Further, to ensure the pruning effect, these rectangular areas should fully cover  $M(T_q)$ . Such a rectangular spatial area can be obtained by expanding the spatial range of each dimension of  $M(T_q)$  by using  $d$ . Assuming that the coordinates of the lower left corner and the upper right corner of  $M(T_q)$  are  $(x_{q1}, y_{q1})$  and  $(x_{q2}, y_{q2})$ , respectively. Therefore, the coordinates of the lower left corner and upper right corner of  $M_1(T_q, d)$  are  $(x_{q1} - d, y_{q1})$  and  $(x_{q2} + d, y_{q2})$ , and the coordinates of the lower left corner and upper right corner of  $M_2(T_q, d)$  are  $(x_{q1}, y_{q1} - d)$  and  $(x_{q2}, y_{q2} + d)$ . It is easy to know that  $M_1(T_q, d)$  and  $M_2(T_q, d)$  are fully covered by  $R(T_q, d)$ , and  $M(T_q)$  is fully covered by them. Hence, we obtain Pruning strategy 2.

**Pruning strategy 2.** Given a query trajectory  $T_q$ , a distance threshold  $d$ , a *drtree* node  $N_d$  which has passed the check by Pruning strategy 1. If  $(M(N_d) \cap M_1(T_q, d)) \cup (M(N_d) \cap M_2(T_q, d)) \neq \emptyset$ , then the value of Mindist between  $M(N_d)$  and  $M(T_q)$  is not greater than  $d$ . Otherwise, we should calculate  $\text{Mindist}(M(N_d), M(T_q))$  to determine whether pruning  $N_d$ .

For example, in Figure 4, nodes  $N_3$  and  $N_5$  overlap with  $M_1(T_q, d)$ , they need not be pruned, while nodes  $N_2$  and  $N_4$  do not overlap with  $M_1(T_q, d)$  and  $M_2(T_q, d)$ , and it is necessary to further calculate the value of Mindist to decide whether pruning  $N_2$  and  $N_4$ .

In summary, we name this method which combines Pruning strategy 1 and Pruning strategy 2 as Extended MBR overlap based pruning strategy (EMOB pruning strategy), Algorithm 1 gives its detailed flow. This algorithm is triggered when traversing each *drtree* node  $N_d$ . If the return value is true, then  $N_d$  should not be pruned. Otherwise,  $N_d$  should be pruned. The general flow of the algorithm is as follows:

1. The algorithm first determines whether the time interval of  $N_d$  overlaps with the time interval of  $T_q$ . If there is overlap between the two, the algorithm will perform the next step, and return false otherwise (line 1 to 3).
2. Whether  $M(N_d)$  overlaps with  $M(R(T_q, d))$  is checked. If any exist, the algorithm will continue to the next step. Otherwise, the false is returned (line 4 to 6).
3. The algorithm judges whether  $M(N_d)$  overlaps with  $M_1(T_q, d)$  or  $M_2(T_q, d)$ . If no overlaps exist, the next step will be performed. Otherwise true is returned (line 7 to 9).
4. Whether the value of  $Mindist(M(N_d), M(T_q))$  is not larger than  $d$  is checked. The return value is true if  $Mindist(M(N_d), M(T_q)) \leq d$ . Otherwise false is returned (line 10 to 14).

---

**Algorithm 1. EMOB Pruning Strategy**


---

**Input:** Query trajectory  $T_q$ , *drtree* node  $N_d$ , Distance Threshold  $d$ ;

**Output:** The true value means retaining  $N_d$ , the false value means pruning  $N_d$ ;

```

1  if  $TS(N_d) \cap TS(T_q) = \emptyset$  then
2    return false;
3  endif
4  if  $M(N_d) \cap M(R(T_q, d)) = \emptyset$  then
5    return false;
6  endif
7  if  $(M(N_d) \cap M_1(T_q, d)) \cup (M(N_d) \cap M_2(T_q, d)) \neq \emptyset$  then
8    return true;
9  endif
10 if  $Mindist(M(N_d), M(T_q)) > d$  then
11   return false;
12 else
13   return true;
14 endif

```

---

As with the basic pruning strategy, EMOB pruning strategy is also valid when any sub-trajectory of  $T_q$  is used as the pruning reference object. Hence, our method is suitable for higher precision pruning occasions. In Section 4.3, we will apply EMOB pruning strategy in the best-first traversal algorithm.

#### 4.2. E3DR-Tree

Compared with the pruning method with taking the whole query trajectory as the pruning reference object, the pruning method with taking each trajectory segment of it as the reference one can obtain more accurate pruning results. This is because the invalid space of the MBRs which enclose the trajectory segments is less than that of the MBR which encloses the whole trajectory. For example, in Figure 5, the  $Mindist$  between the MBR of *drtree* node  $N_1$  and  $M(T_q)$  is smaller than  $d$ , but the  $Mindists$  between the MBR of the  $N_1$  and the MBRs of the trajectory segment  $l_1$  is greater than  $d$ . Therefore,  $N_1$  does not satisfy the candidate requirement of  $l_1$ , and it is not necessary to calculate the distance between any trajectory segments contained in  $N_1$  and  $l_1$  in the refinement step.

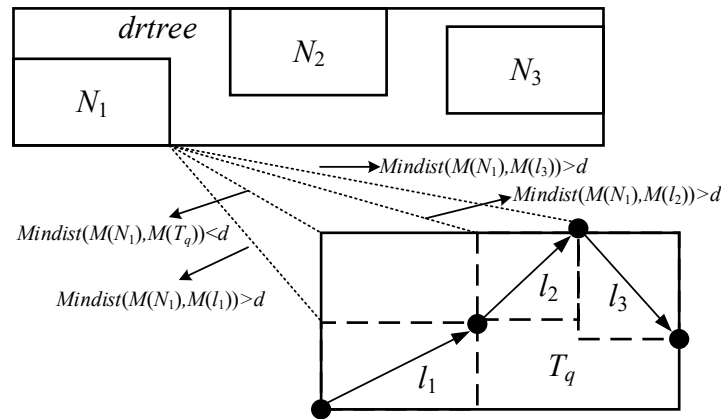


Figure 5. Example of Mindists of different data granularities.

Although the trajectory segment-based method can improve the pruning precision, in the pruning process, it is necessary to traverse the *drtree* once for each trajectory segment of  $T_q$ , resulting in a large increase in node traversal overhead. In order to reduce the node traversal overhead, we also organized all the trajectory segments contained in  $T_q$  by a spatiotemporal index called *qrtree*. In the pruning step, *drtree* and *qrtree* are traversed at the same time, this makes it possible to generate a precise pruning result without having to traverse the *drtree* multiple times, thus effectively reducing the overhead of traversing the nodes. The traversal algorithm will be discussed separately in Section 4.3, this section first describes the index structure used by *qrtree*.

*Qrtree* uses an index structure called the Extended 3DR-tree (E3DR-tree). An example of the structure of E3DR-tree is shown in Figure 6. The difference between E3DR-tree and the traditional 3DR-tree is shown in three aspects:

1. Node selection condition. Whenever a trajectory segment is inserted, the node with the smallest change in the time interval is selected as the inserted node.
2. Node split processing. When a node needs to be split, while balancing the number of child nodes included in the new nodes, it is also necessary to ensure that the time intervals of new nodes have no overlap.
3. The child nodes (or trajectory segments) of a node are sorted in the ascending order of the start timestamp of the corresponding time interval.

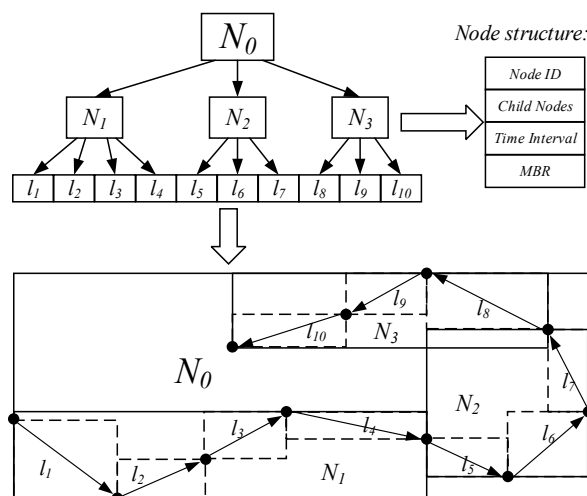


Figure 6. Example of E3DR-tree.

Although the construction of E3DR-tree does not consider the spatial factor directly, for the trajectory data of the same moving object, the trajectory segments that are close in time are usually close in space, so E3DR-tree still has a strong spatial distinguishing ability. Moreover, E3DR-tree ensures that the trajectory segments can be processed in chronological order during traversal, which is consistent with their order in the trajectory so that the overhead of the subsequent sorting processing can be effectively reduced.

#### 4.3. Best-First Traversal Algorithm

We designed a best-first traversal algorithm that traverses *drtree* and *qrtree* simultaneously to handle the pruning process. Compared to the pruning method that traverses *drtree* alone, it can generate an accurate result with accessing fewer nodes. Its basic principle is to select the accessed objects of the next iteration according to the heights of the accessed *drtree* node and the *qrtree* node. As the number of iterations increases, the pruning precision continues to rise, a set of candidate trajectory segments is eventually generated for each trajectory segment of  $T_q$ .

To support the best-first traversal algorithm, we use a first priority queue (FirstPQ) and multiple secondary priority queues (SecPQ) to record the intermediate results during the traversal process [18]. FirstPQ is used to control the traversal order of the *qrtree* nodes, and SecPQ is used to control the traversal of the *drtree* nodes. First, the data structures of FirstPQ entry (F-entry) and SecPQ entry (S-entry) are introduced.

**Definition 3.** Attributes of each F-entry ( $N_q, h_q, t_q, SPQ$ ) are described as follows:

- (1) Node  $N_q$ —a *qrtree* node, which can be an index node or a trajectory segment;
- (2) Height  $h_q$ —the height from  $N_q$  to the trajectory segment layer of *qrtree*. if  $h_q = 0$ , then  $N_q$  is a trajectory segment. In addition, the F-entries in a FirstPQ are sorted by  $h_q$  value (largest to smallest).
- (3) Timestamp  $t_q$ —the starting timestamp of the time interval of  $N_q$ . In addition,  $t_q$  is the secondary keyword for sorting F-entries, when two F-entries have the same  $h_q$  value, they are sorted by  $t_q$  value (smallest to largest).
- (4) SecPQ  $SPQ$ —a SecPQ that records the *qrtree* nodes which pass the pruning check with  $N_q$ .

**Definition 4.** Attributes of each S-entry ( $N_d, h_d, t_d$ ) are described as follows:

- (1) Node  $N_d$ —a *drtree* node, which can be an index node or a trajectory segment;
- (2) Height  $h_d$ —the height from  $N_d$  to the trajectory segment layer of *drtree*. if  $h_d = 0$ , then  $N_d$  is a trajectory segment. In addition, the S-entries in a SecPQ are sorted by  $h_d$  value (largest to smallest).
- (3) Timestamp  $t_d$ —the starting timestamp of the time interval of  $N_d$ . In addition,  $t_d$  is the secondary keyword for sorting S-entries, when two S-entries have the same  $h_d$  value, they are sorted by  $t_d$  value (smallest to largest).

Algorithm 2 gives its detailed flow of the best first traversal algorithm, it is divided into two steps of initialization (lines 1 to 8) and iteration (lines 9 to 19) and using a collection  $Ps$  to collect all pruning results.

In the initialization step, an E3DR tree *qrtree* is first created for the query trajectory  $T_q$  (line 1). A SecPQ  $SPQ$  and a FirstPQ  $FPQ$  are then initialized (lines 2 to 3). Next, the root nodes of *qrtree* and *drtree* are obtained, and the pruning check is performed. If the root node of *drtree* is not be pruned, an S-entry and an F-entry are created and inserted in  $SPQ$  and  $FPQ$ , respectively. Otherwise, the algorithm ends (lines 4 to 8).

For each iteration of the while loop, the first F-entry  $fe_1$  is dequeued from  $FPQ$ , and the head S-entry  $se_1$  of the  $fe_1.SPQ$  is also checked without dequeuing (lines 10 to 11). Based on the values of  $fe_1.h_q$  and  $se_1.h_d$ , a decision is made whether to traverse *qrtree*, to traverse *drtree* or to add a pruning result to  $Ps$ , the processing of the three cases are as follows:

- Case 1 (At least one of  $fe_1.h_q$  and  $se_1.h_d$  is not 0, and  $fe_1.h_q \geq se_1.h_d$ ): The child nodes of  $fe_1.N_q$  are traversed by the function TRA-Q( $FPQ, fe_1, d$ ), and when each child node is accessed, the pruning check is performed for the *drtree* node of each S-entry in  $fe_1.SPQ$  (lines 12 to 13). The pseudo code of the function TRA-Q( $FPQ, fe_1, d$ ) is shown in Algorithm 3.
- Case 2 (At least one of  $fe_1.h_q$  and  $se_1.h_d$  is not 0, and  $fe_1.h_q < se_1.h_d$ ): The child nodes of  $se_1.N_d$  are traversed by the function TRA-D( $FPQ, fe_1, d$ ), and the pruning check is performed when each child node is accessed (lines 14 to 15). The pseudo code of the function TRA-D( $FPQ, fe_1, d$ ) is shown in Algorithm 4.
- Case 3 (Both of  $fe_1.h_q$  and  $se_1.h_d$  are 0): Namely both of  $fe_1.N_q$  and  $se_1.N_d$  are the trajectory segments. Moreover, according to the ordering rule of SecPQ, the *drtree* node of any S-entry in  $fe_1.SPQ$  is also a trajectory segment and is a candidate of  $fe_1.N_q$ . Therefore,  $fe_1$  can be regarded as a pruning result and added to  $Ps$  (line 16 to 17).

---

**Algorithm 2.** Best-First Traversal Algorithm
 

---

**Input:** Query Trajectory  $T_q$ , distance threshold  $d$ , *drtree*;

**Output:** Pruning results  $Ps$ ;

```

1  qrtree ← Create an E3DR-tree for trajectory  $T_q$ ;
2  SPQ ← initialize an instance of SecPQ;
3  FPQ ← initialize an instance of FirstPQ;
4   $N_d \leftarrow \text{Root}(\textit{drtree})$ ;
5   $N_q \leftarrow \text{Root}(\textit{qrtree})$ ;
6  if EMOB( $N_d, N_q, d$ ) = true then
7    SPQ.enqueue( $(N_d, H(N_d), TS(N_d))$ );
8    FPQ.enqueue( $(N_q, H(N_q), TS(N_q), SPQ)$ );
9    while FPQ  $\neq \emptyset$  do
10      $fe_1 \leftarrow \textit{FPQ.dequeue}()$ ;
11      $se_1 \leftarrow fe_1.SPQ.\text{getFirst}()$ ;
12     if  $(fe_1.h_q \neq 0 \vee se_1.h_d \neq 0) \wedge (fe_1.h_q \geq se_1.h_d)$  then
13       TRA-Q(FPQ,  $fe_1, d$ );
14     else if  $(fe_1.h_q \neq 0 \vee se_1.h_d \neq 0) \wedge (fe_1.h_q < se_1.h_d)$  then
15       TRA-D(FPQ,  $fe_1, d$ );
16     else if  $fe_1.h_q = 0 \wedge se_1.h_d = 0$  then
17       Ps.add( $fe_1$ );
18     endif
19   endwhile
20 endif
21 return Ps;

```

---

In the function TRA-Q( $FPQ, fe_1, d$ ), for each child node  $C_q$  of the node  $fe_1.N_q$ , the following processing is performed:

1. Initialize a SecPQ CSPQ (line 2);
2. Loop read each S-entry of  $fe_1.SPQ$  (without dequeuing), let *cse* be the current read S-entry if *cse.N<sub>d</sub>* is not pruned, then *cse* is inserted into CSPQ (lines 3 to 7).
3. Create a new F-entry for  $C_q$  by using the relevant parameters and insert it into *FPQ* (line 8).

**Algorithm 3.** TRA-Q( $FPQ, fe_1, d$ )**Input:** FirstPQ  $FPQ$ , F-entry  $fe_1$ , distance threshold  $d$ ;**Output:** Null;

```

1  for each child node  $C_q$  of  $fe_1.N_q$  do
2     $CSPQ \leftarrow$  initialize an instance of SecPQ;
3    for each entry  $cse$  of  $fe_1.SPQ$  do
4      if  $EMOB(cse.N_d, C_q, d) = \text{true}$  then
5         $CSPQ.enqueue(cse)$ ;
6      endif
7    endfor
8     $FPQ.enqueue((C_q, H(C_q), TS(C_q), CSPQ))$ ;
9  endfor

```

The process of the function TRA-D ( $FPQ, fe_1, d$ ) is as follows:

1. Dequeue the head S-entry  $se_1$  from  $fe_1.SPQ$  (line);
2. Traverse the child nodes of  $se_1.N_d$ , and perform the pruning check for each child node  $C_d$ , if  $C_d$  is not pruned, then an S-entry is created for  $C_d$  and inserted into  $fe_1.SPQ$  (line 2 to 6);
3. Insert  $fe_1$  into  $FPQ$  again (line 7).

**Algorithm 4.** TRA-D( $FPQ, fe_1, d$ )**Input:** FirstPQ  $FPQ$ , F-entry  $fe_1$ , distance threshold  $d$ ;**Output:** Null;

```

1   $se_1 \leftarrow fe_1.SPQ.dequeue()$ ;
2  for each child node  $C_d$  of  $se_1.N_d$  do
3    if  $EMOB(C_d, fe_1.N_q, d) = \text{true}$  then
4       $fe_1.SPQ.enqueue(C_d, H(C_d), TS(C_d))$ ;
5    endif
6  endfor
7   $FPQ.enqueue(fe_1)$ ;

```

The best-first traversal algorithm ends when there are no F-entries in  $FPQ$ . According to the F-entry structure, each entry of  $Ps$  records a query trajectory segment of  $T_q$  and a set of candidate trajectory segments, and the entries of  $Ps$  are sorted based on the chronological order of the query trajectory segment, so in the refinement step, the entries of  $Ps$  will be processed naturally in chronological order, thereby effectively reducing the processing overhead of sorting. Compared with the method of pruning *drtree* nodes with taking the whole query trajectory as the pruning reference object, the best priority traversal algorithm can generate more accurate candidate results and reduce the overhead required for the refinement step. In addition, because our method adopts the strategy of traversing *drtree* and *qrtree* at the same time, it ensures that the *drtree* is not traversed multiple times in the case of obtaining a high-precision pruning results, so the cost of accessing the index nodes is greatly reduced.

After the pruning step is finished, the candidate trajectory segments need to be refined to obtain the final results. Since the focus of our study is pruning optimization, the refinement step is only briefly explained here, and the detailed process of the refinement step of the historical continuous query can be found in the literature [6]. In the pruning result  $Ps$ , for each trajectory segment  $l_q$  of  $T_q$ , assume that one of its candidate trajectory segments is  $l_d$ . First,  $l_d$  is interpolated to obtain the time interval  $ti_q$  that overlaps with that of  $l_q$ . Then the distance between  $l_d$  and  $l_q$  at any time instance in  $ti_q$  is calculated, the square of this distance is a quadratic expression with time as the parameter. Next, the distance threshold  $d$  is brought into the expression to obtain a quadratic equation inequality, this inequality is solved to obtain a time interval  $ti_c$  where the distance between  $l_d$  and  $l_q$  is less than  $d$ . If  $ti_q$  overlaps

with  $ti_c$  (naming the overlap time Interval as  $ti_o$ ), then the moving object  $l_d.oid$  is a query result of  $ti_o$ . After all the data of  $Ps$  is processed, all the query results are returned to the user, and the query ends.

#### 4.4. Performance Analysis

The time complexity of the best-first traversal algorithm comes from the processes of creating the E3DR-tree and iterative searching. Suppose that the query trajectory  $T_q$  and the moving object database  $D$  contain respectively  $n$  and  $m$  trajectory segments. First, in the aspect of creating the E3DR-tree, since the E3DR-tree is created in the same way as the traditional R-tree, the running time of creating it is  $O(n \log n)$ . Second, in the aspect of iterative searching, all candidate trajectory segments are concentrated on just one leaf node of the *drtree* in the best case, so the time complexity is  $O(n + \log m)$ . Conversely, in the worst case, each trajectory segment in  $T_q$  needs to match each trajectory segment in  $D$ , it takes  $O(mn)$  rounds of computation. Certainly, it is difficult to achieve the theoretical worst-case complexity when actually performing iterative searching. In summary, the total time complexity of the best-first traversal algorithm is  $O(n \log n + \log m)$  to  $O(n \log n + mn)$ .

Figure 7 shows an example of the pruning process of THC query, where  $T_q$  contains six trajectory segments, each trajectory in  $D$  contains four trajectory segments, and the distance threshold  $d$  is one. The maximum number of children of a node in the 3DR-tree that indexes  $T_q$  or  $D$  is three. Considering that there are not many trajectory segments in the example, we do not consider the time attribute, and only performed pruning based on the spatial distance.

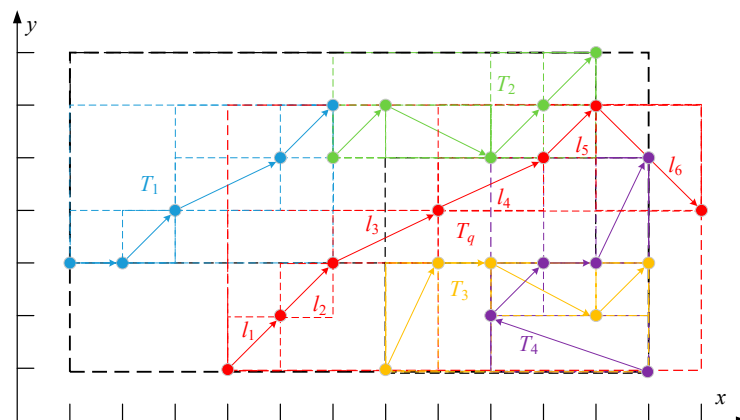


Figure 7. Example of the pruning process of THC query.

The best first traversal algorithm (shorted as BFT) takes a total of 105 pruning checks to get the pruning results, in which the number of pruning is 100 times by checking the overlap between the MBRs, and the number of pruning is only five times by checking the Mindist. As a comparison, the pruning method proposed in literature [10] that takes each segment of the query trajectory as a reference object (shorted as TDS) takes 114 pruning checks, while the pruning method proposed in literature [12] (shorted as CDQLTD) that regards the whole query trajectory as the pruning reference takes only 31 pruning checks. From the pruning results shown in Table 2, benefiting from the segment-based pruning way, the pruning results of TDS and BFT are closer to the final results than that of CDQLTD. Moreover, compared to TDS, due to the pruning strategy that combines MBR overlap and Mindist calculation, the pruning accuracy achieved by BFT is more than that of TDS.

**Table 2.** Comparison of pruning results.

Trajectory Segment	Candidate Quantity (BFT)	Candidate Quantity (TDS)	Candidate Quantity (CDQLTD)
$l_1$	0	1	15
$l_2$	2	2	15
$l_3$	8	10	15
$l_4$	10	11	15
$l_5$	4	4	15
$l_6$	6	7	15

## 5. Experiment

### 5.1. Experimental Set Up

In order to verify the effectiveness of our pruning optimization method, we implemented it in Java and verified in the Linux environment. For the experiment, a PC (Intel Xeon E5-2620 V2, 16GB memory, 2TB disk) running Ubuntu 16.04 64-bit was used.

The experiments used the global AIS (Automatic Identification System) [19] data from 1 July to 5 July 2012 as the data source, in which each AIS message was regarded as a spatial location of a moving object at a timestamp. We randomly extracted some data from the data source to form five datasets. The statistical information is shown in Table 3. When constructing a 3DR-tree for a dataset during the experiment, it was considered that the motion track between the spatial positions with a long time interval may be significantly different from the real motion track, according to the maximum transmission time interval of the AIS message, we made the following provisions: If an AIS message had an adjacent message within six minutes of the time interval, the motion track between the spatial positions of the two messages was taken as a trajectory segment. Otherwise, it was regarded as a special trajectory segment with the same start time and end time. We evaluated the performance of BFT with TDS [10] and CDQLTD [12]. The query performances were evaluated under different data scales, different time ranges and different distance thresholds. The evaluated metrics included the following four aspects:

1. Number of the accessed nodes: The sum of the number of index nodes and the number of trajectory segments checked during pruning;
2. Selectivity: The ratio of the number of candidate trajectory segments obtained by pruning to the number of trajectory segments contained in the dataset;
3. Pruning Latency: The execution time of the pruning step during a query;
4. Query Latency: The execution time of a query.

**Table 3.** Statistics of Datasets.

Name	No. of Moving Objects	No. of AIS Messages
AIS01	73,490	10,000,000
AIS02	95,732	20,000,000
AIS03	110,566	40,000,000
AIS04	136,932	80,000,000
AIS05	152,807	160,000,000

For each experiment, we performed 50 queries, and used the average as the experiment result. By default, we used AIS05 as the experimental dataset, 24 h as the query time range, and two nautical miles as the distance threshold.

## 5.2. Performance of Different Data Scales

In this part of the experiments, datasets AIS01, AIS02, AIS03, AIS04, and AIS05 were used as experimental data to evaluate the query performance of the three methods under different scales, as shown in Figure 8.

It can be seen from Figure 8a,b that as the data scale increases, the number of accessed nodes increases in the pruning step. However, the increase rate of the pruning results is smaller than the change of data scales, so the selectivity is gradually decreasing. Among the three methods, CDQLTD has the fewest number of the accessed nodes, because it uses a single MBR of the whole query trajectory as the pruning reference, and the spatiotemporal index of the dataset only needs to be traversed once. However, CDQLTD has the lowest pruning precision, and the pruning results contain some irrelevant data, so CDQLTD has the worst selectivity. While TDS uses each trajectory segment of the query trajectory as the reference, it is necessary to repeatedly traverse the spatiotemporal index of the dataset, and the number of the accessed nodes is one order of magnitude larger than the two methods. However, it also benefits from the segment-based pruning way, the pruning results of TDS is closer to the final query results, so its selectivity performance is better than that of CDQLTD. BFT also uses each query trajectory segment as the pruning reference, but thanks to the E3DR-tree structure and the best-first traversal algorithm, the number of the accessed node is much smaller than that of TDS. Moreover, the pruning strategy adopted by BFT combines MBR overlap and Mindist calculation, so the selectivity performance of BFT is better than that of TDS which only consider MBR overlap.

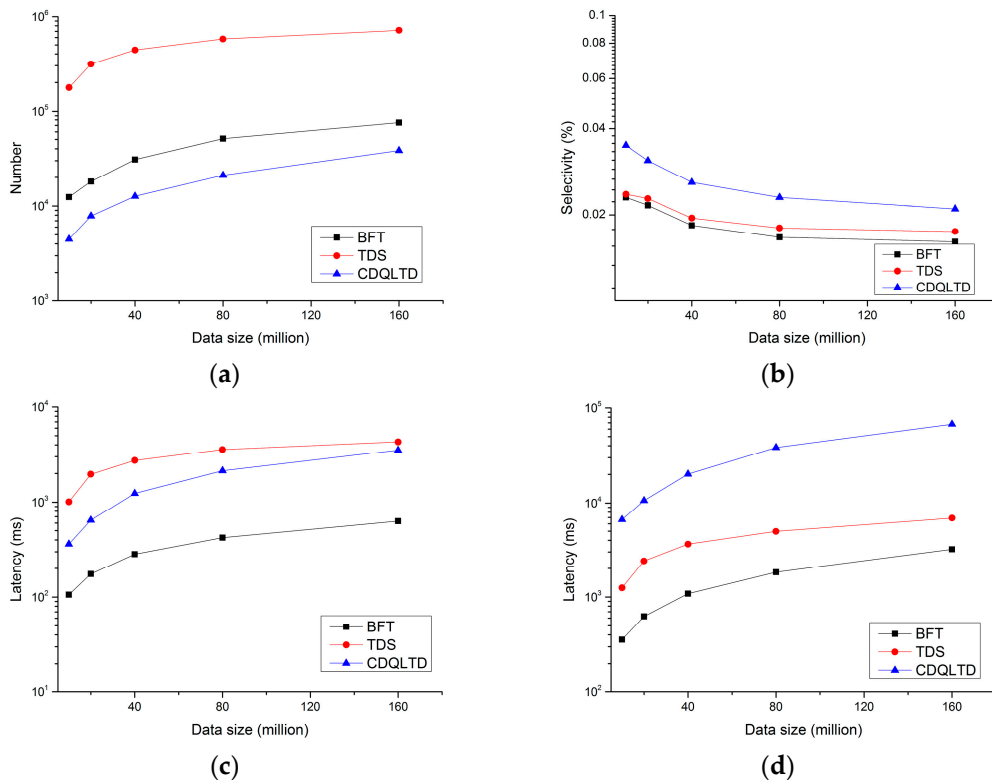


**Figure 8.** Performance of different scales: (a) Number of the accessed nodes, (b) selectivity, (c) pruning latency, (d) query latency.

Figure 8c shows the performance of pruning latency. Since BFT accesses fewer nodes and its pruning strategy based on extended MBR overlap effectively reduce the time overhead of a single pruning check, so BFT takes less time than the two methods. Although CDQLTD visits the fewest nodes when pruning, the calculation process of pruning check based on Mindist is complex and time-consuming, resulting in a large time overhead for the entire pruning process. TDS has the lowest

time-consuming pruning check method, but the number of the accessed nodes is much more than the two methods, resulting in the most time-consuming pruning.

The performance of query latency is shown in Figure 8d, where BFT performs best, not only because BFT takes the least time to complete the pruning step, but also generates the highest precision of pruning results, so the process of refinement also takes the least time. The pruning results of CDQLTD have the lowest precision, which makes it necessary to spend a lot of time on refinement processing, the time difference between it and the two methods will be further amplified as the data scale increases.

### 5.3. Performance of Different Time Ranges

Figure 9 shows the query performance of the three different methods at different time ranges. It can be seen from Figure 9a that as the query time range increases, the number of candidates involved also increases, and all three methods need to access more nodes to obtain candidates. Figure 9b shows that the change in selectivity is proportional to the change in the time range, this is because the increase in the number of candidate segments will naturally increase the selectivity when the data size is constant. As shown in Figure 9c,d, since all three methods require more time to generate and process the candidate segments, their pruning latency and query latency increase with the increase of time range. Among the three methods, BFT has the best query performance. In all cases, BFT takes less than eight seconds to complete the query process, while the time spent by CDQLTD gradually increases from 34 s to 134 s. The reason for this difference in performance has been explained in Section 5.2, it will not be described in detail here.

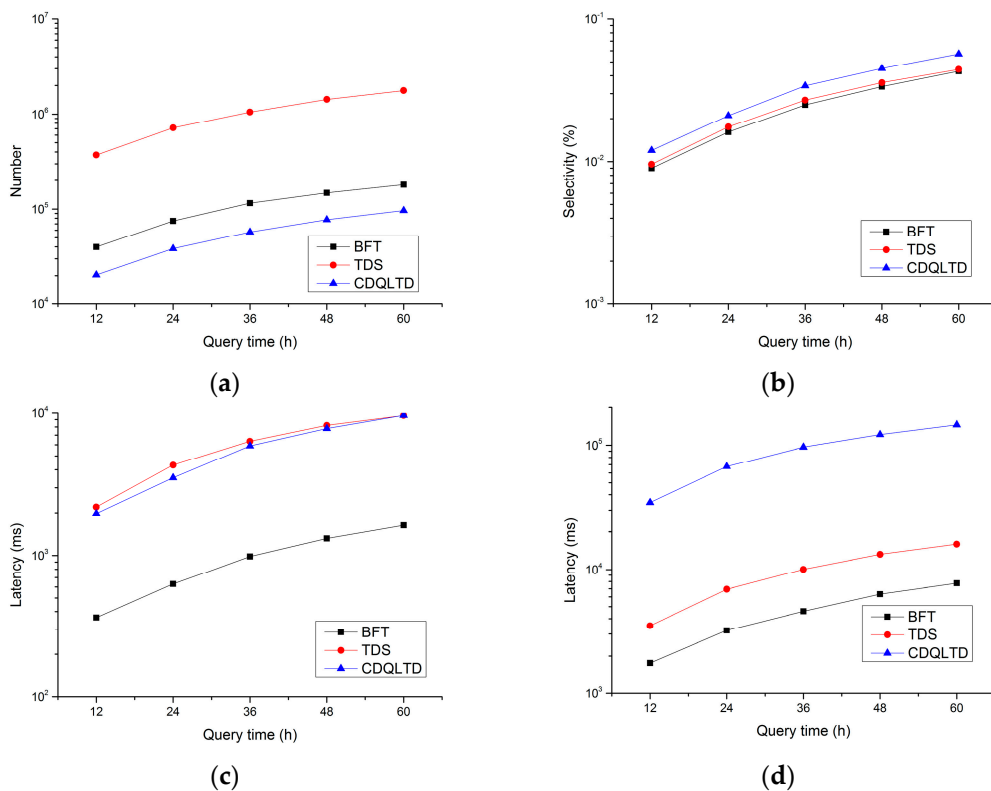


**Figure 9.** Performance of different time ranges: (a) Number of the accessed nodes, (b) selectivity, (c) pruning latency, (d) query latency.

### 5.4. Performance of Different Distance Thresholds

This part of the experiments evaluated the query performance of different distance thresholds, as shown in Figure 10. As the distance threshold increases, the query spatial range of query increases, and

the increased speed shows an increasing trend. It causes more index nodes and trajectory segments to be accessed and checked, and the pruning results contain more candidates. As shown in Figure 10a,b, the growth rate of the number of accessed nodes, and that of selectivity will also increase. Naturally, when the distance threshold is increased from one nautical mile to five nautical miles. It can be seen from Figure 10c,d that the pruning latency and query latency of the three methods also increases. Among them, the performance of BFT is still better than that of the other two. In terms of pruning latency, it takes less than one-fifth of the two methods. In terms of query latency, it takes less than half of that of TDS, and is an order of magnitude smaller than that of CDQLTD.

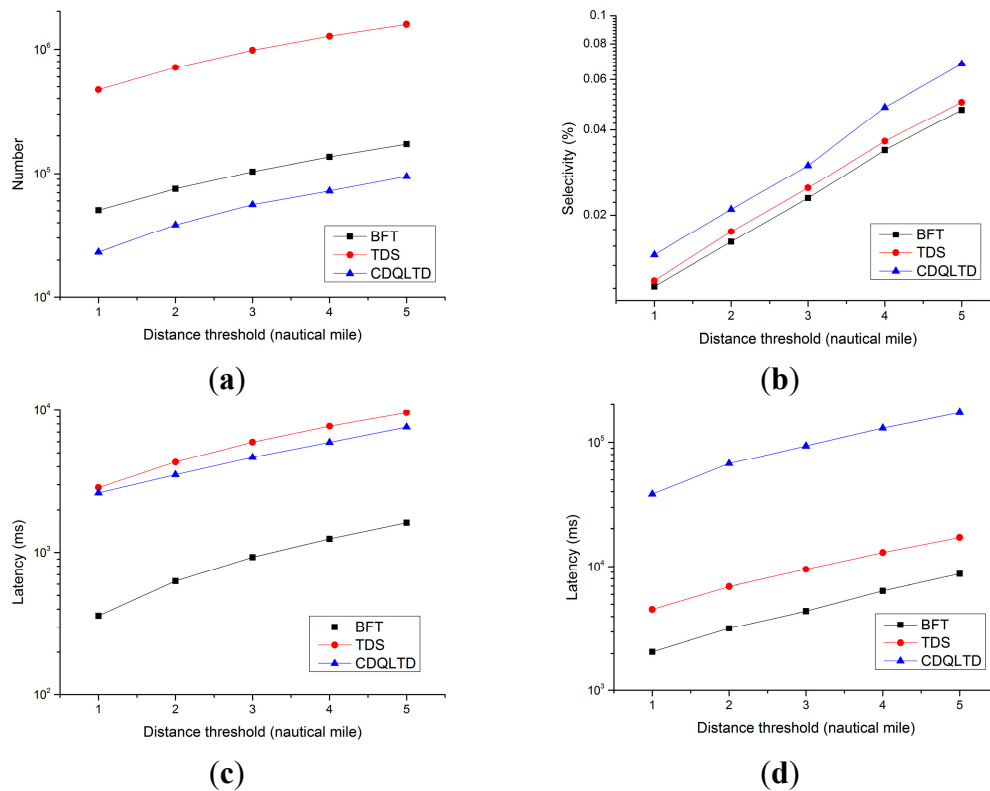


**Figure 10.** Performance of different distance thresholds: (a) Number of the accessed nodes, (b) selectivity, (c) pruning latency, (d) query latency.

### 5.5. Summary of the Experiments

In order to measure the performance of our pruning method, we conducted the above experimental study based on a real dataset. Regarding the historical continuous queries, it has been shown that the best-first traversal algorithm always has better performance of selectivity rate and query latency compared with the other two methods in all cases. This is because the pruning accuracy and the number of accessed nodes are considered comprehensively in our method. Moreover, we demonstrated that our improvement over the pruning strategy can sufficiently increase the performance of the proposed algorithms, compared with CDQLTD method, it achieves less pruning latency in the case of accessing more nodes.

## 6. Conclusions

We studied a specific sub-domain of the continuous queries of moving objects, namely the pruning optimization of historical continuous queries based on a threshold. First, we optimized the processing overhead of a single pruning check using a pruning strategy based on extended MBR overlap. Secondly, a 3DR-tree extension structure called E3DR-tree was proposed for traversing the query trajectory, and based on this, the best-first traversal algorithm was introduced, so that the accurate pruning results

could be obtained with accessing as few nodes as possible. Finally, a large number of experimental results verify the effectiveness of our method. In the future work, we plan to apply this method to the distributed environment, and combine it with a distributed index, to further improve the query performance based on parallelization techniques. Moreover, we will improve this method to solve another sub-problem of historical continuous query— $k$ -nearest history continuous query.

**Author Contributions:** Conceptualization, J.Q. and Q.L.; data curation, J.Q.; methodology, J.Q.; supervision, L.M.; validation, J.Q. and Q.L.; writing—original draft, J.Q.; writing—review and editing, L.M. and Q.L. All authors have read and approved the final manuscript.

**Funding:** This research was funded by National Natural Science Foundation of China, grant number 61802425.

**Conflicts of Interest:** The authors declare no conflict of interest.

## References

1. Zhang, Z.; Jin, C.; Mao, J.; Yang, X.; Zhou, A. TrajSpark: A Scalable and Efficient In-Memory Management System for Big Trajectory Data. In Proceedings of the Asia-Pacific Web (APWeb) and Web-Age Information Management (WAIM) Joint Conference on Web and Big Data, Beijing, China, 7–9 July 2017.
2. Salmon, L.; Ray, C. Design principles of a stream-based framework for mobility analysis. *GeoInformatica* **2017**, *21*, 237–261. [[CrossRef](#)]
3. Nutanong, S.; Ali, M.E.; Tanin, E.; Mouratidis, K. Dynamic Nearest Neighbor Queries in Euclidean Space. *Encycl. GIS* **2015**, 1–7.
4. Trajcevski, G.; Tamassia, R.; Cruz, I.F.; Scheuermann, P.; Hartglass, D.; Zamierowski, C. Ranking continuous nearest neighbors for uncertain trajectories. *VLDB J.* **2011**, *20*, 767–791. [[CrossRef](#)]
5. Theodoridis, Y.; Vazirgiannis, M.; Sellis, T. Spatio-temporal indexing for large multimedia applications. In Proceedings of the Third IEEE International Conference on Multimedia Computing and Systems, Hiroshima, Japan, 17–23 June 1996.
6. Frentzos, E.; Gratsias, K.; Pelekis, N.; Theodoridis, Y. Algorithms for nearest neighbor search on moving object trajectories. *GeoInformatica* **2007**, *11*, 159–193. [[CrossRef](#)]
7. Papadias, D.; Zhang, J.; Mamoulis, N.; Tao, Y. Query processing in spatial network databases. In Proceedings of the 29th International Conference on Very Large Data Bases, Berlin, Germany, 9–12 September 2003.
8. Pfooser, D.; Jensen, C.S.; Theodoridis, Y. Novel Approaches in Query Processing for Moving Object Trajectories. In Proceedings of the 26th International Conference on Very Large Data Bases, Cairo, Egypt, 10–14 September 2000.
9. Güting, R.H.; Behr, T.; Xu, J. Efficient  $k$ -nearest neighbor search on moving object trajectories. *VLDB J.* **2010**, *19*, 687–714.
10. Gowanlock, M.; Casanova, H. In-memory distance threshold queries on moving object trajectories. In Proceedings of the Sixth International Conference on Advances in Databases, Knowledge, and Data Applications, Chamonix, France, 20–25 April 2014.
11. Dagum, L.; Menon, R. OpenMP: An industry-standard API for shared-memory programming. *CiSE* **1998**, *1*, 46–55. [[CrossRef](#)]
12. Huorong, H.; Jianqiu, X.; Xiaolin, Q. Continuous Distance Queries over Large Trajectory Data. *J. Chin. Comput. Syst.* **2017**, *38*, 2505–2510. (In Chinese)
13. Chakka, V.P.; Everspau, A.; Patel, J.M. Indexing large trajectory data sets with SETI. *CIDR* **2003**, *75*, 76.
14. Gowanlock, M.; Casanova, H. Distance threshold similarity searches on spatiotemporal trajectories using GPGPU. In Proceedings of the 2014 21st International Conference on High Performance Computing (HiPC), Goa, India, 17–20 December 2014.
15. Gowanlock, M.; Casanova, H. Indexing of spatiotemporal trajectories for efficient distance threshold similarity searches on the GPU. In Proceedings of the 2015 IEEE International Parallel and Distributed Processing Symposium, Hyderabad, India, 25–29 May 2015.
16. Gowanlock, M.; Casanova, H. Distance threshold similarity searches: Efficient trajectory indexing on the GPU. *IEEE Trans. Parallel Distrib. Syst.* **2016**, *27*, 2533–2545. [[CrossRef](#)]
17. Mahmood, A.R.; Punni, S.; Aref, W.G. Spatio-temporal access methods: A survey (2010–2017). *GeoInformatica* **2019**, *23*, 1–36. [[CrossRef](#)]

18. Nutanong, S.; Jacox, E.H.; Samet, H. An Incremental Hausdorff Distance Calculation Algorithm. *Proc. VLDB Endow.* **2011**, *4*, 506–517. [[CrossRef](#)]
19. Harati-Mokhtari, A.; Wall, A.; Brooks, P.; Wang, J. Automatic Identification System (AIS): Data reliability and human error implications. *J. Navig.* **2007**, *60*, 373–389. [[CrossRef](#)]



© 2019 by the authors. Licensee MDPI, Basel, Switzerland. This article is an open access article distributed under the terms and conditions of the Creative Commons Attribution (CC BY) license (<http://creativecommons.org/licenses/by/4.0/>).